

## Dynamic fracture toughness measurements in composites by instrumented Charpy testing: influence of aging

A. Fernández-Canteli<sup>a,\*</sup>, A. Argüelles<sup>a</sup>, J. Viña<sup>a</sup>, M. Ramulu<sup>b</sup>, A.S. Kobayashi<sup>b</sup>

<sup>a</sup>Department of Construction and Manufacturing Engineering, University of Oviedo, 33204 Gijón, Spain

<sup>b</sup>Department of Mechanical Engineering, Box 352600, University of Washington, Seattle WA, 98195, USA

Received 19 April 2001; received in revised form 24 January 2002; accepted 3 April 2002

### Abstract

The dynamic behavior of three different fiber fabric composite laminates was studied by testing notched specimens in an instrumented Charpy machine. The registered impact force and displacement at the specimen hammer contact point were used to evaluate Mode-I fracture energy and dynamic fracture toughness. The changes in fracture toughness due to impact velocity, crack size and stacking sequence of the specimen were investigated with different degrees of aging conditions. Aging was found to significantly affect the dynamic fracture toughness, but had less effect on the static fracture toughness.

© 2002 Elsevier Science Ltd. All rights reserved.

*Keywords:* Fabric composites

### 1. Introduction

Composites are used extensively in aerospace as well as commercial structures applications due to their high strength-to-weight ratio. However, a constant concern is the effect of foreign object impacts, which can severely damage and degrade the strength of composite structures. Therefore, the dynamic fracture behavior of fiber reinforced composite materials under impact loads is of significant practical importance in terms of their service performance. The many aspects of impact response of fiber reinforced polymer matrix composites have received the attention of a large number of investigators during the past decade [1–3]. Excellent reviews of the composite studies on the dynamic properties in composites using instrumented Charpy tests and low-velocity impact tests were reported recently in Refs. [4–8]. Krinke et al. [9], who studied notched and unnotched Charpy test specimens, provided an insight into the inherent differences between observed static and dynamic failure modes. Kalthoff [10] and Chamis and Sinclair [11], on the other hand, have investigated the impact energy

absorption and the relevant mechanisms. Nevertheless, when compared with dynamic failure research in metals, little advance has been made in the corresponding research in composites. In fact, considering the attempts made 20 years ago to relate dynamic fracture toughness to the dynamic results of notched bend tests of metallic specimens [3], it is reasonable to conclude that no noticeable advances have occurred since that time. With increasing applications of composites as structural members and mechanical components exposed to dynamic loading, a better knowledge of their dynamic properties is urgently needed [2,12]. One of the main and unsolved questions is to find suitable and acceptable tests with representative results that can be applied to design. First and utmost, the dynamic loading test must be relevant to the dynamic loading encountered in the real structural member.

Since standard techniques used for static fracture characterization of metals seem applicable to composites, it may be reasonable to apply these to the dynamic domain, particularly the use of the instrumented Charpy hammer [5,8,12]. In doing so, the uncertainties in the Charpy testing of metals are inherently carried into Charpy testing of composites. In addition, the application of linear elastic fracture mechanics (LEFM) for isotropic and homogeneous materials to the static and dynamic fracture characterization of composites is

\* Corresponding author. Tel.: +34-98-5182054; fax: +34-98-5182055.

*E-mail address:* canteli@charpy.edv.uniovi.es  
(A. Fernández-Canteli).

questionable since composites are nonhomogeneous, often orthotropic, materials. Even on a macroscopic scale, the mechanisms of fracture differ markedly from those of metals. Nevertheless, it could be argued that, on a microscopic scale, the same non-homogeneity should also be considered for the metals. Thus, the similarity between the force displacement Charpy outputs obtained for composites and for metallic materials justifies the use of this phenomenological approach for obtaining the dynamic fracture toughness.

It is hoped that an experimental study will achieve some qualitative, if not quantitative, progress in the knowledge of the dynamic fracture behavior of composites under impact loading at the intermediate impact velocity of 1–5 m/s. The purpose of this investigation is, therefore, to explore the possibility of applying the instrumented Charpy impact technique in order to determine the dynamic fracture toughness,  $K_{I_d}$ , in carbon and glass fiber fabric composites for comparison with the corresponding static value,  $K_{I_c}$ . The influences of notch size, impact velocity and specimen arrangement as well as that of aging have been considered and the conclusions are extrapolated to a more general validity. Therefore, the dynamic fracture parameters so obtained are regarded as provisional experimental data with questionable applicability for practical cases until more conclusive validation tests can be performed.

## 2. Experimental procedure and methodology

### 2.1. Materials

The materials used were three different commercially available fiber textile composites. The first composite (CTEA-10), is made of an epoxy resin reinforced with carbon fiber textile, arranged as a 2/2 twill weave, by Hercules Aerospace España S.A. The material was

acquired as a 2 mm thick laminate and stacked to the desired laminate thickness. The second composite (CTPO-7), arranged as a 8H satin, is made of a high performance thermoplastic resin PEI (polyetherimide) reinforced with carbon fiber textile. This material was supplied by the manufacturer as a laminate with a final thickness of 7 mm. The third material (VTPO-5), also arranged as a 8H satin, is made of a PEI reinforced with glass fiber textile, type E, manufactured by Ten Cate Advanced Composites. This material was delivered as a prepreg roll, which was stacked to a thickness of 5 mm for curing. A hot-dish press POLYSTAT 300S with a curing cycle as recommended by the manufacturer, was used. The mechanical properties for the three materials used in this investigation are summarized in Table 1.

### 2.2. Specimen shape and fabrication

The PEI specimens were produced by direct piling of the prepreg to the desired thickness (7 mm for the CTPO composite, or 5 mm for the VTPO, respectively). In the case of the carbon–epoxy CTEA composite, the specimens were stacked with the original 2 mm thick laminate. In order to study the influence of specimen preparation (Fig. 1), three different laminae stackings were considered:

Table 1  
Mechanical properties of the three materials used

	CTEA-10	CTPO-7	VTPO-5
Tensile strength (MPa)	795	544	310
Flexural modulus (GPa)	–	45	20
Young's modulus (GPa)	68.5	62	25
Shear strength (MPa)	90	–	–
Volumetric fraction (%)	57	58	67

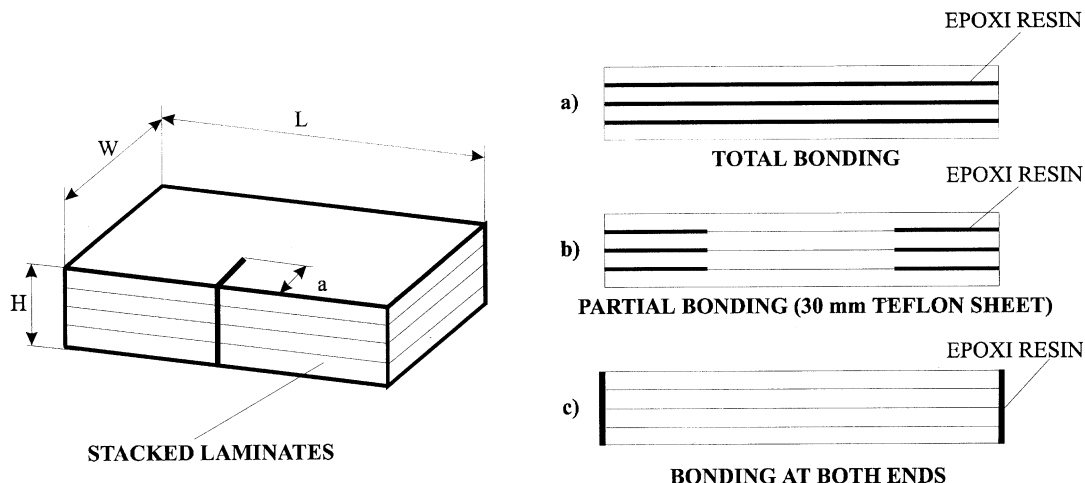


Fig. 1. Geometry and different preparation of the specimens.

- Full bonding with epoxy resin as adhesive between the different laminae (Fig. 1a).
- Bonding of the laminae with an adhesive except along 30 mm in the middle region of the specimen where teflon sheets had been placed between the laminae (Fig. 1b).
- Bonding at the two edges of the specimen (Fig. 1c).

The thickness was held constant along each of the three composites and was large enough to avoid lateral buckling of the specimens during impact loading and subsequent failure. The specimens were aged by immersion in the humid corrosive atmosphere of an environmental chamber Vötsch VC-2020, for 6–210 days, with a relative humidity of 95% and a temperature of 70 °C. This environment represented approximately, the environmental conditions encountered by a composite vessel used in the paper and pulp industry. A 0.5 mm notch was made using a radial disc saw. Unlike metals, in which a unique initial crack is induced by fatigue loading, composites under fatigue develop a damage region around the notch tip. Thus, fatigue pre-cracking of the specimens was not used in this series of experiments. Previous experimental studies [12] had shown that the notch geometry has no significant influence on the instrumented Charpy test results. However, a clean and sharp notch, made by a cutter, leads to less scattering of results.

### 2.3. Procedure and methodology

Impact tests were carried out using a conventional IBERTEST PIB-30 Charpy hammer with a maximum impact energy of 300 J, instrumented under the guidance of J.F. Kalthoff of the Ruhr-Universität Bochum, Germany. The static tests were carried out in a MTS 810.22 dynamic machine with a load capacity of 100 KN.  $K_{Ic}$  was calculated according to ASTM E399 [13], which is valid for metals. For the determination of  $K_{Ia}$ , the quasi-static approach suggested by a tentative standard, ASTM E24.03.03 [14], was used. This tentative ASTM standard is based on the direct estimation of the maximum fracture load by the force transducer located on the striker of the Charpy hammer with prescribed restrictions. Although the minimum time which elapsed during fracture or the minimum energy at fracture were intended for metallic materials in the elastic or in the plastic range, no specific standard applicable to composites has been developed to date. Thus, the feasibility of applying both standards is also an object of this study.

In an instrumented Charpy impact test [12,15,16] the loading force  $F(t)$  acting on the tup of the striking hammer during the failure process is measured by means of strain gages placed on the tup. After suitable conversion it is possible to express the force as a function of deflection:

$$s(t) = \int_0^t v_0 - \left(\frac{1}{m}\right) \int_0^t F(t) dt$$

or

$$F(s) = \frac{d}{dt} \left[ m \left( v_0 - \frac{ds(t)}{dt} \right) \right]$$

where:

- $s$ : deflection of the specimen at the impact point
- $v_0$ : initial impact velocity of the pendulum
- $m$ : mass of the pendulum
- $F$ : registered force
- $t$ : time elapsing from the beginning of loading

The work done or the energy consumed for a given deflection is computed as:

$$W(s) = \int_0^s F(s) ds$$

Fig. 2 shows two representative, idealized curves for both ductile and brittle materials in which the characteristic points of the loading force ( $F_{gy}$ ,  $F_m$ ,  $F_{iu}$ ,  $F_a$ ) and deflections ( $S_{gy}$ ,  $S_m$ ,  $S_{iu}$ ,  $S_a$ ) are indicated. The meanings of the subscripts are:

- $gy$ : beginning of total yielding in the ligament or, alternatively, end of the linear loading force range
- $m$ : maximum value
- $iu$ : beginning of unstable crack propagation
- $a$ : end of unstable crack propagation

The choice of loading force or impact energy as a scale parameter for calculating the dynamic fracture toughness has been suggested [17] and has been adopted for this study. For the procedure to be applicable to the materials considered, the same restrictions for metals were imposed namely:

- (1) Failure must initiate before generalized damage occurs. This is guaranteed if the force-displacement relations for  $F_{iu}/2$  and for  $F_{iu}$  differ by less than 10%.
- (2) The time which elapses at failure must be long enough for the oscillations to be sufficiently damped. This is assumed to occur if  $t_{iu} > 3\tau$ , where  $\tau$  is the natural vibration period of the specimen. The tentative ASTM standard gives an approximate formula for estimating  $\tau$  for isotropic materials. For this non-homogeneous, anisotropic specimen,  $\tau$  was determined through a direct observation of the oscillation in the force-deflection curve. The high number of oscillations observed in the load-deflection curves of

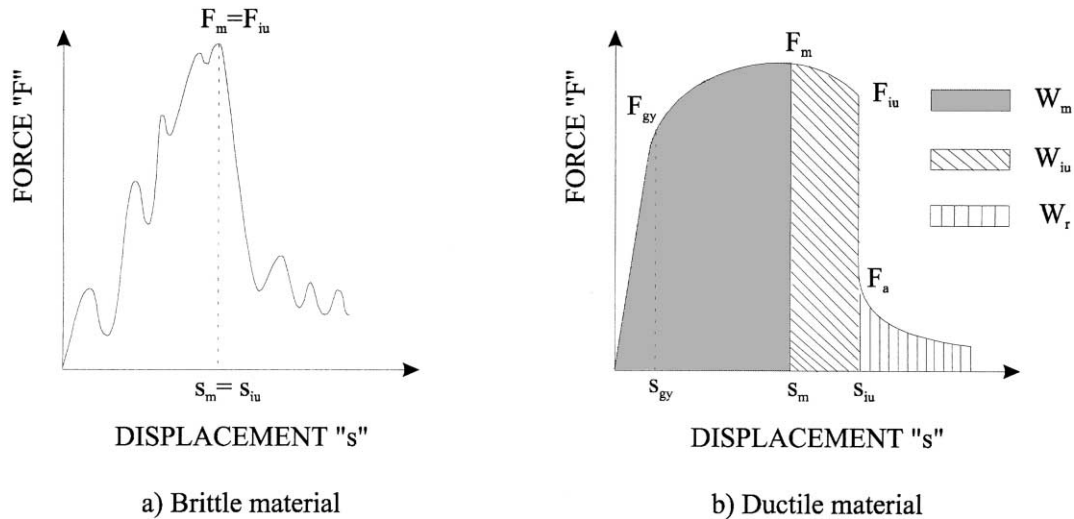


Fig. 2. Idealized force-displacement Charpy curves.

the three materials indicates that  $t_{iu} > 3\tau$  condition was satisfied.

- (3) A complete failure process occurs only at high hammer velocity, such that the potential energy supplied at the onset of the impact is at least three times the energy consumed during the failure process.
- (4) A further requirement concerning the straight crack front (no tunneling), which is pertinent for metals, may not be applicable here. With a

material which exhibits elastic linear behavior to a brittle fracture, the specimen can be considered to have failed before a generalized damage sets in. According to ASTM E 24.03.03 [14], the dynamic fracture toughness,  $K_{Id}$ , can then be calculated from the critical value of the load, i.e., from the load measured just at the beginning of the unstable fracture, using the conventional expression derived for the static stress intensity factor. Due to the linear relation between force

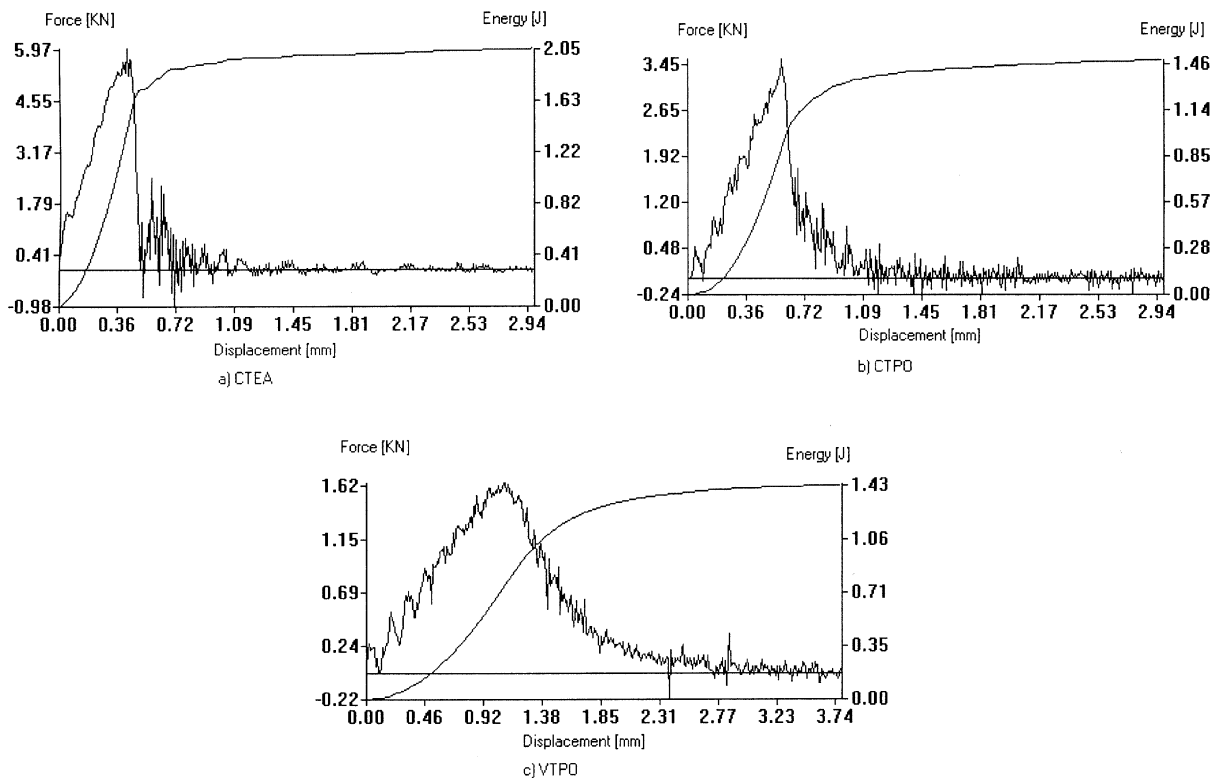


Fig. 3. Force-displacement curves for the materials studied ( $V=2.5$  m/s, 70 days in aging chamber).

and energy, a direct equivalence exists between the two quantities. The approach proposed by ASTM 24.03.03 for metals consists of determining the maximum force,  $F_m$ , the maximum displacement,  $s_m$  and the time which elapses,  $t_m$ . If  $F_m$  is assumed to be identical with  $F_{iu}$ , i.e. as the force which indicates the beginning of unstable crack propagation, the dynamic fracture toughness,  $K_{Id}$ , assuming a linear-elastic behavior, can be represented as [14]:

$$K_{Id} = (F_{iu}S/BW^{3/2})[2.9(a_m/W)^{1/2} - 4.6(a_m/W)^{3/2} + 21.8(a_m/W)^{5/2} - 37.6(a_m/W)^{7/2} + 38.7(a_m/W)^{9/2}]$$

where,

- $F_{ui}$ : force by crack instability
- $B$ : specimen thickness
- $W$ : specimen width
- $S$ : span between supports
- $a_m$ : notch length

If the material exhibits some ductile behavior (a progression of continuous damage could be described as pseudo-plastic) accompanied by unstable growth of the crack, then the specimen is considered to have failed after the presence of generalized damage. The ASTM E 992 procedure [13] for steels with unstable fracture determines an equivalent fracture toughness,  $[K_{Id}]_{eq}$ , deduced from the equivalent force to its maximal value.  $[F_{iu}]_{eq}$ , which is linearly related to the displacement, would consume the same failure energy. Thus, the same expression as presented above for the calculation of fracture toughness could be used in our study. However, the determination of the maximum force, which indicates the start of a stable crack growth, is, in general, cumbersome, so the J-integral should be used to characterize the fracture toughness, as in static cases. In the present case, with a relatively small rounding-off of the force-displacement curves, a rough estimation of the maximum load was made to avoid the above mentioned difficulties. Finally, the fractographic analysis of the fractured specimens was carried out using scanning electron microscopy. Some post-fracture analysis of the

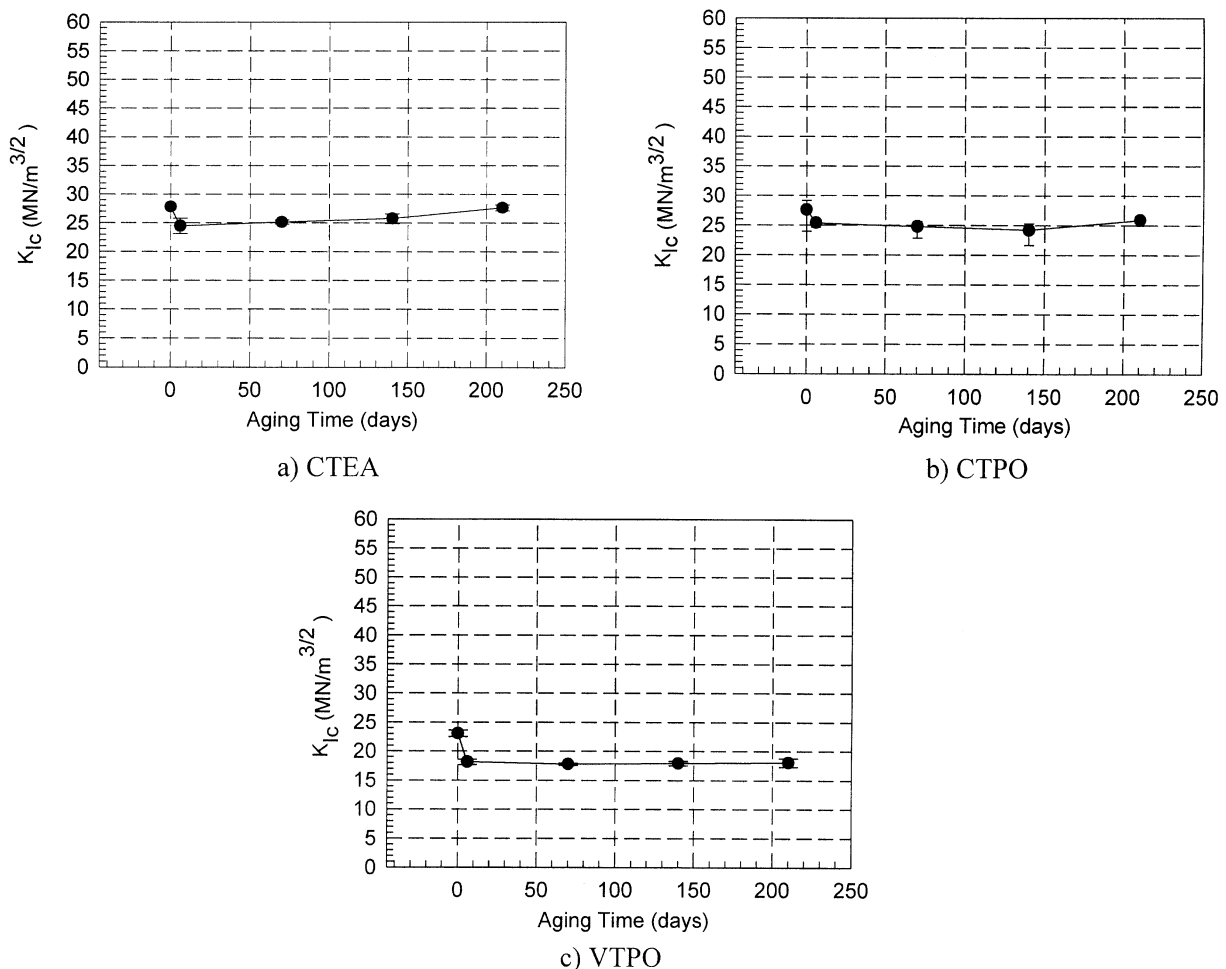


Fig. 4. Static fracture toughness,  $K_{Ic}$ , as a function of aging time.

specimens are presented to elucidate the failure process under dynamic loading.

### 3. Results

Fig. 3 shows the typical force-displacement curves for three composite materials, namely CTEA, CTPO, and VTPO at an impact velocity of 2.5 m/s, and after being aged for 70 days. Note that the load applied was recorded during the entire fracture process of the specimen. In the case of the CTEA specimen, failure was brittle fracture. Before the generalized damage occurred, the CTEA specimen failed (Fig. 3a). However, composite specimens with CTPO and VTPO exhibited a continuous damage progression prior to failure. The force-displacement records (Fig. 3b and c) depict certain round-out in the transition zone to the failure and the fall of the load is not so abrupt as in the case of CTEA material. Thus, the maximum force cannot easily be identified.

#### 3.1. Static fracture toughness

Fig. 4 shows the static fracture toughness as a function of the aging time in the three materials obtained for tests under strain control by a motion rate of  $10^{-4}$  m/s, according to [13]. The figures show that the static fracture toughness decreased at the initial stage of aging and was constant as the aging time increased.

#### 3.2. Dynamic fracture toughness

Dynamic fracture toughness,  $K_{I,d}$ , as a function of the impact velocity for constant aging time, is plotted in Fig. 5.  $K_{I,d}$  is fairly insensitive to the impact velocity of  $v = 1.4\text{--}5.4$  m/s although a slight increase of  $K_{I,d}$  is noted at higher impact velocities. Within the experimental conditions, the impact velocity appears to have only a minor effect on the dynamic fracture toughness. The results confirmed that the test requirements were met and, consequently, justified the calculation of  $K_{I,d}$ , using the formulae for quasi-static failure given by ASTM

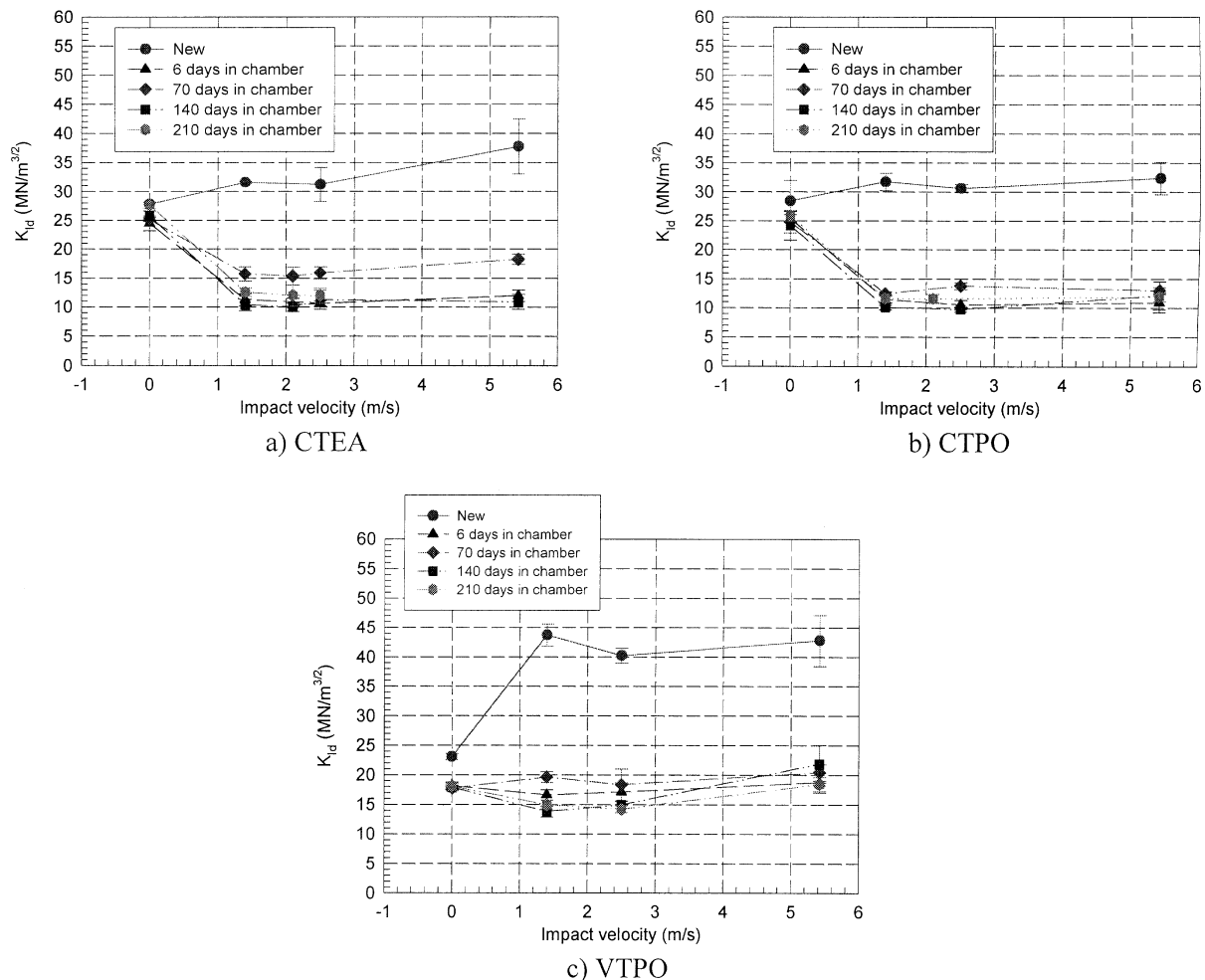


Fig. 5. Dynamic fracture toughness,  $K_{I,d}$ , as a function of impact velocity for given aging time.

24.03.03. However, aging has a significant effect on the dynamic fracture toughness for a given impact velocity. This effect is clearly shown in Fig. 6, in which the fracture toughness is plotted as a function of the aging time for given impact velocities.  $K_{I_d}$  underwent a drastic reduction, and reached a stationary value of about one

third the  $K_{I_d}$  of an intact material of nearly 140 days. The results and their trends are consistent irrespective of the material tested. Dynamic fracture toughness as a function of the normalized notch length for a given aging time for the two composites CTPO and VTPO is shown in Fig. 7. The tests in this series of experiments

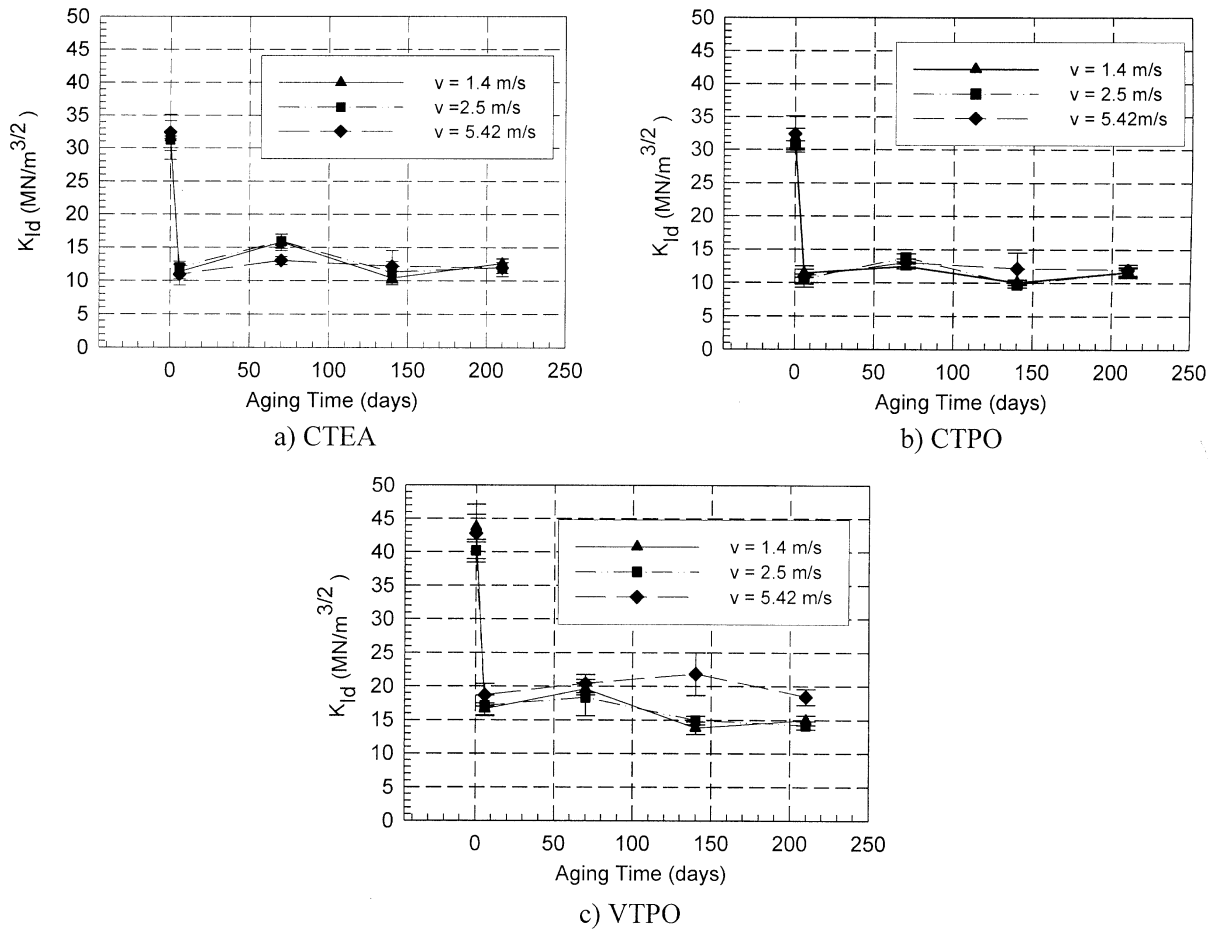


Fig. 6. Dynamic fracture toughness,  $K_{I_d}$ , as a function of aging time for given impact velocity.

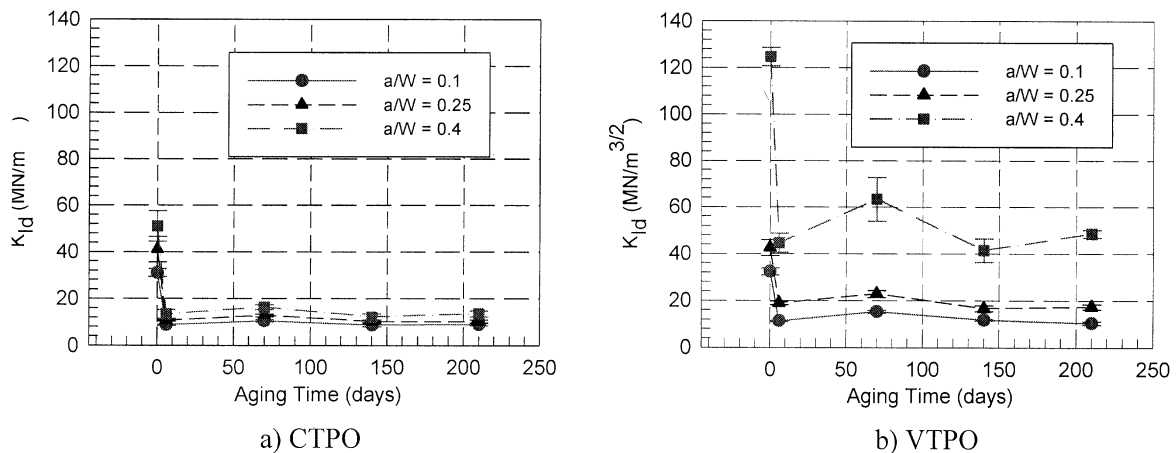


Fig. 7. Dynamic fracture toughness,  $K_{I_d}$ , as a function of notch length for given aging time ( $V=2$  m/s).

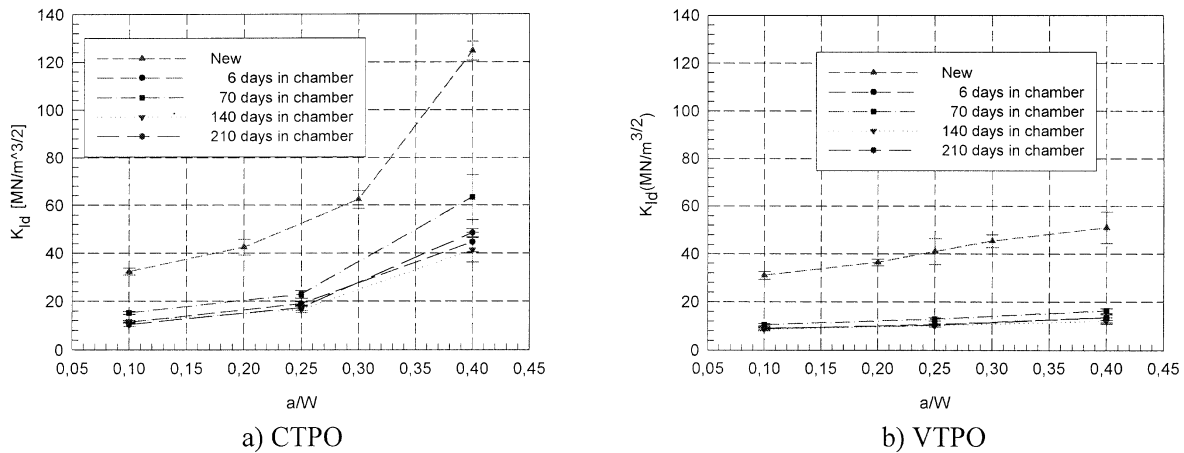


Fig. 8. Dynamic fracture toughness,  $K_{IId}$ , as a function of aging time for given notch length ( $V=2$  m/s).

were conducted with an impact velocity of 2 m/s using CTPO and VTPO composites.  $K_{IId}$  increases with increasing notch length  $a/W$  for  $a/W=0.1-0.4$ . The effect is far more perceptible in material VTPO for which  $K_{IId}$  seems to follow a growth law with a very steep slope. For material CTPO it can be concluded that, in the  $a/W$  range considered, the growth law is approximately linear. This trend holds for all aging times. Similar increases in the fracture toughness have been observed numerically [18] and experimentally [19].

The dynamic fracture toughness as a function of aging for a given notch length is shown in Fig. 8. Note that the  $K_{IId}$ , increased with the increase in notch length and significantly decreased with aging. For all the different aging times, Fig. 8 shows an initial dramatic reduction of  $K_{IId}$  for all the notch lengths up to about one third of the fracture toughness measured at the intact specimens. Since this reduction is reached in less than 6 days, it indicates that the aging process happens in a very short time, after which the value of  $K_{IId}$  remains stationary. For material VTPO,  $K_{IId}$  oscillates during the aging time process for the longest notch size, with an apparent mild rise by 70 days. This is not accidental since it is present in both materials for all notch lengths and for all preparations of the specimen. In order to evaluate the effect of the variation in processing of the CTEA composite specimens, the dynamic fracture toughness data is plotted as a function of the aging for three different preparations of the specimens is shown in Fig. 9. The impact velocity used in this series of tests was 2 m/s. The  $K_{IId}$ , regardless of processing methods, clearly degraded as soon as it was aged. For the three different preparations (Fig. 3), no influence of the preparation of the specimen can be observed for CTEA. The same dependence of  $K_{IId}$  with the aging time as in the previous case can be stated, i.e. a large drop to about a third of the value for new material and endurance with increasing aging in the first days.

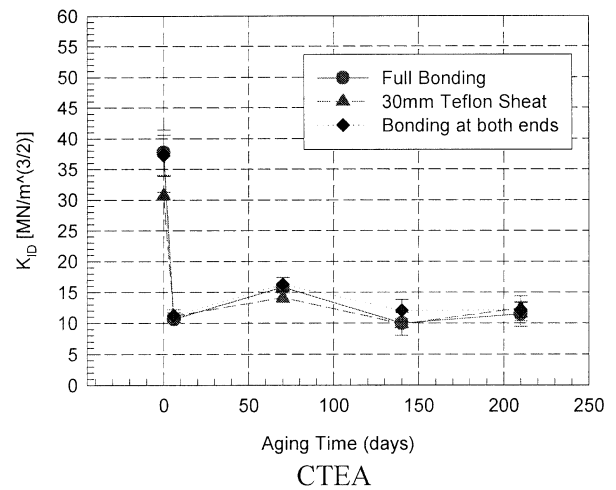


Fig. 9. Dynamic fracture toughness,  $K_{IId}$ , as a function of notch length for given aging time ( $V=2$  m/s).

### 3.3. Fractographic analysis of the failures

Due to the high complexity of the failure process in the Charpy test, scanning electron microscopy was used to analyze all the fractured samples in the close vicinity of the notch. Fig. 10 shows a comparison of the fracture zones, close to the initial notch line in CTEA, CTPO and VTPO composites. The carbon-epoxy (CTEA) composite fracture shows the brittle nature of the material, with carbon fibers breaking predominantly in the same failure plane, with limited fiber pullout as shown in Fig. 10a–c. No conclusive information can be obtained concerning the matrix failure, although brittle matrix cracking was always associated with multiple fragmentation of fibers. The rough appearance of the fiber surface indicates a good bonding between fiber and matrix. The fiber failure surface was found to be very irregular and rough.

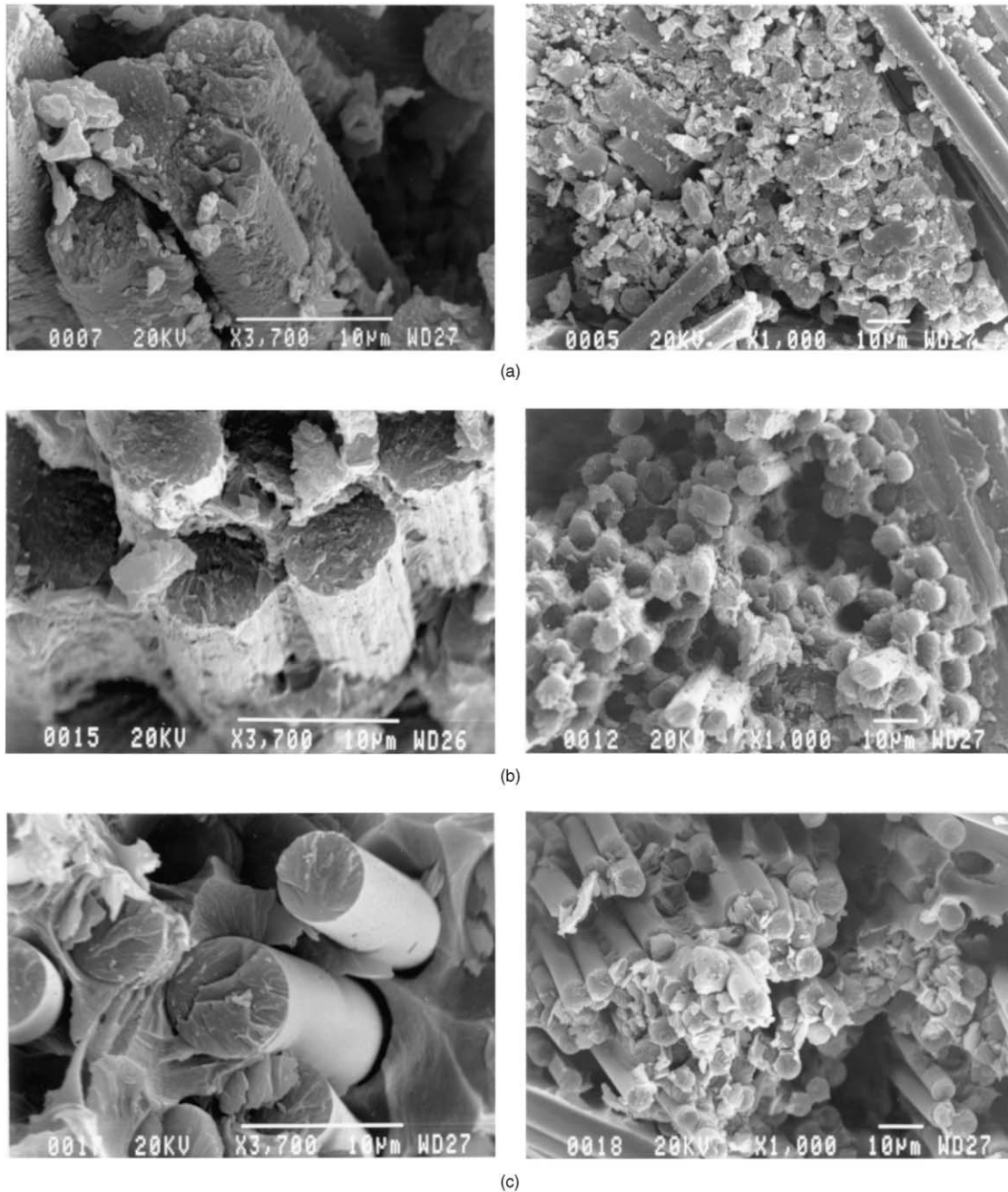


Fig. 10. View of specimen fracture close to the initial notch for the three materials studied ( $\times 3700$  and  $\times 1000$ ).

Failure in the carbon–PEI (CTPO) composite occurred in different planes within the fracture surface, presenting a rough surface with rapidly changing valleys and peaks due to the characteristic fiber pullout holes. The matrix clearly failed without fragmentation. The bonding strength between the matrix and the fiber is increased by the grooved or striated surface of the fibers, and is in contrast with the glassy fiber surface. This is a likely reason for the absence of looseness between the fiber and the matrix, thus minimizing the pull-out process. Failure results in a cross section, with

slight irregularities, in a plane perpendicular to the fiber axis.

In the glass–PEI (VTPO) composite, the pull-out of the glass fiber is even more conspicuous than in the former case, showing greater differences in the height of the broken fibers or depth of the holes. Fiber failure takes place in bundles of fibers which, together with the smooth surface of the fiber pull-out and the looseness of their outer boundary in the embedding matrix (see black spaces between fibers and holes), indicates a lack of adhesion and resulting pull-out failure. The failure in

the matrix is clean, extending to broader areas than in the other cases. The failure cross section shows typical cleavage steps, predominantly perpendicular to the fiber axis, but sometimes showing a moderate inclination.

#### 4. Discussion

The force-displacement records obtained by the instrumented Charpy test and shown in Fig. 3 justify its use as a possible method for characterizing composites under dynamic loading. The critical point lies in the interpretation and limited application of these results. The observation of the instrumented Charpy output graphics, and the SEM micrographs of the fractured surfaces shown in Fig. 10 indicates that the nature of failure was an ideal brittle failure for the carbon-epoxy composite (CTEA), brittle failure with some ductile features in the case of the carbon-PEI composite (CTPO), and ductile failure, with no perceptible plastic straining, in the glass-PEI composite (VTPO). As regards the static fracture toughness, only the influence of aging was considered here. Qualitatively (Fig. 8), the static fracture toughness,  $K_{Ic}$ , shows a similar dependence on aging as the dynamic fracture toughness, experiencing a reduction at a very early stage followed by a constant toughness with increasing aging time (Fig. 9). Some signs of recovery could be assumed in the material CTEA, although they could be considered to fall within the expected scatter range. The values of the static fracture toughness,  $K_{Ic}$ , agreed reasonably well with those found for the dynamic fracture toughness,  $K_{Id}$ , for the composite CTEA, and still better for the composite CTPO for the different aging conditions. In the case of the composite VTPO, the static fracture toughness obtained was 50% lower than the dynamic fracture toughness for new material. No differences were found to exist between the values for both  $K_{Ic}$  and  $K_{Id}$  for aged material.

#### 5. Conclusions

The force-displacement curves obtained by the instrumented Charpy test justify its use as a possible method for characterizing the composites under dynamic loading. The critical point however, lies in the interpretation and limited application of these results, considering the variability in the micro-mechanics of failure. Based on this exploratory experimental study of dynamic fracture toughness measurement in composites using the instrumented Charpy test, the following conclusions were made:

1. The dynamic fracture toughness exhibited significant reduction in value under aggressive environmental conditions as a function of the aging time, especially at early

stages; this result should be taken into account in the design of real structures. On the other hand, the impact velocity exerts no noticeable influence on the magnitude of the dynamic fracture toughness for different ages.

2. The static fracture toughness of the composites under study shows no evidence of being influenced by aging, although its value for the studied materials can be of the same order (CTEA, CTPO) or much lower than the dynamic fracture toughness (VTPO) approaching the value for aged material.

3. The dynamic and the static fracture toughnesses increase with the crack growth for the two composite materials considered. While material CTPO was not sensitive to the notch size, the VTPO shows a considerable increase of the toughness with increasing notch size. Again, aging does not exert any noticeable influence on the results for the two materials. In this case the dynamic fracture toughness represents only a small fraction of about 30% of the static fracture toughness.

4. The preparation of the specimens does not play a significant role concerning either the static or the dynamic fracture toughness. As a result, stacking the laminae by simply gluing the ends is a suitable enough way of preparing the specimens.

5. While aging significantly affects the results of the dynamic fracture toughness, it has less effect on the static fracture toughness. This should be clarified by a suitable investigation of the microstructure of the material.

#### References

- [1] Abrate S. Impact on composite structures. New York: Cambridge University Press; 1998.
- [2] Sierakowski RL, Chaturvedi SK. Dynamic loading and characterization of fiber-reinforced composites. New York: John Wiley; 1997.
- [3] CSNI Specialist Meeting on Instrumented Precracked Charpy Testing. Palo Alto, Ca. 1–3 December, 1980, EPRI NP-2102-LD, Project 1757-1, CSNI No. 67 Proceedings; November 1981.
- [4] Adams DF. Impact response of polymer-matrix composite materials. composite materials: testing and design. ASTM STP 617, Philadelphia; 1977. p. 409–426.
- [5] Blackman BRK, Williams JG. Impact and high rate testing of composites: an overview. In: Proceedings of the NATO Advanced Study Institute on Mechanics of Composite Materials and Structures. NATO Science series; 1999. Vol. 361, p. 215–224.
- [6] Blackman BRK, Williams JG. Impact and high rate testing of composites: high rate delamination testing. In: Proceedings of the NATO Advanced Study Institute on Mechanics of Composite Materials and Structures. NATO Science series; 1999. Vol. 361, p. 225–234.
- [7] Richardson MOW, Wisheart MJ. Review of low-velocity impact properties of composite materials. Composites Part A 1996;27: 1123–31.
- [8] Sims GD, Understanding Charpy impact testing of composite laminates. Proceedings of the 6th International Conference on Composite Materials 1988;3:3.494–3.507.
- [9] Krinke DC, Barber JP, Nicholas T. The Charpy impact test as a method for evaluating impact resistance of composite materials. Dayton, OH: AFML TR 78–54; 1978.

- [10] Kalthoff JF. On the validity of impact energies measured with polymeric specimens in instrumented impact tests. In: Williams JG, Pavan A, editors. *ESIS 19*. London: Mechanical Engineering Publications; 1995. p. 21–31.
- [11] Chamis CC, Sinclair JH. Impact resistance of fiber composites: energy-absorbing mechanisms and environmental effects. *ASTM STP 864*. Philadelphia; 1985. p. 326–45.
- [12] Tan L. Determining fracture dynamics parameters by means of instrumented charpy impact technique [in Spanish]. PhD thesis, University of Oviedo, Department of Construction and Manufacturing Engineering; 2000.
- [13] ASTM E 399/81. Standard method for plane strain fracture of metallic materials; 1981.
- [14] ASTM E 24.03.03. Proposed standard method of test for instrumented impact testing of precracked charpy-specimens of metallic materials; 1980.
- [15] Fernández-Canteli A, Arguelles A, Tan L, Kalthoff JF. Fracture dynamic behavior of composites: influence of thickness and impact rate [in Spanish]. *Anales de Mecánica de la Fractura* 1998; 15:285–90.
- [16] Kalthoff JF. Fundamentals for the assessment of data measured by impact tests using notched and precracked Charpy specimens [in German]. Internal Report. Experimentelle Mechanik, Ruhr-Universität Bochum; 1996.
- [17] Delfosse D, Poursartip A. Energy-based approach to impact damage in CRFP laminates. *Composites Part A* 1997;28A:647–55.
- [18] Lee LJ, Wang CH. Stress intensity factors by weight function method for cracked composite materials. *Eng Fracture Mechanics* 1994;48(2):267–79.
- [19] Srivastava VK. Effect of fibre angle on fracture properties of unidirectional flyash filled FRP. *Eng Fracture Mechanics* 1992; 43(6):1093–6.